Cancer Research

Genes Predisposed to DNA Hypermethylation during Acquired Resistance to Chemotherapy Are Identified in Ovarian Tumors by Bivalent Chromatin Domains at Initial Diagnosis

Edward Curry[1], Constanze Zeller[1], Nahal Masrour[1], Darren K. Patten[1], John Gallon[1], Charlotte S. Wilhelm-Benartzi[2], Sadaf Ghaem-Maghami[1], David D. Bowtell[3], and Robert Brown[1,4]

Abstract

Bivalent chromatin domains containing both active H3K4me3 and repressive H3K27me3 histone marks define gene sets poised for expression or silencing in differentiating embryonic stem (ES) cells. In cancer cells, aberrantly poised genes may facilitate changes in transcriptional states after exposure to anticancer drugs. In this study, we used ChIP-seq to characterize genome-wide positioning of H3K4me3- and H3K27me3-associated chromatin in primary high-grade serous ovarian carcinomas and in normal ovarian surface and fallopian tube tissue. Gene sets with proximal bivalent marks defined in this manner were evaluated subsequently as signatures of systematic change in DNA methylation and gene expression, comparing pairs of tissue samples taken from patients at primary presentation and relapse following chemotherapy. We found that gene sets harboring bivalent chromatin domains at their promoters in tumor tissue, but not normal epithelia, overlapped with Polycomb-repressive complex target genes as well as transcriptionally silenced genes in normal ovarian and tubal stem cells. The bivalently marked genes we identified in tumors before chemotherapy displayed increased promoter CpG methylation and reduced gene expression at relapse after chemotherapy of ovarian cancer. Overall, our results support the hypothesis that preexisting histone modifications at genes in a poised chromatin state may lead to epigenetic silencing during acquired drug resistance.

Significance: These results suggest epigenetic targets for intervention to prevent the emergence of cancer drug resistance. *Cancer Res; 78(6); 1383–91. ©2018 AACR.*

Introduction

Genetic information is packaged into human cells in the form of chromatin: double-stranded molecules of DNA wrapped around complexes of histone proteins. Covalent modifications of the histone tails can alter the density of compaction of chromatin, which can influence the accessibility of DNA to the transcription machinery that is required for gene expression. The Polycomb repressive complex (PRC2), suppresses target gene expression through catalyzing the trimethylation of Lysine 27 of the histone protein H3 (H3K27me3; ref. 1). This modified histone forms broad domains that are enriched at repressed genes (2). PRC2-null mouse embryonic stem (ES) cells can be derived, but do not contribute to viable organisms, so it is widely accepted that PRC2 and H3K27me3 play an important role in the differentiation of pluripotent cells. In ES cells, genomic loci bound by the core PRC2 members (SUZ12, EED, and EZH2) tend to display both the repressive mark H3K27me3 and permissive mark H3K4me3 (trimethylation of Lysine 4 of the histone protein H3). These "bivalent" promoters, simultaneously containing both active and repressive histone marks, are strongly enriched for genes whose expression either rapidly increases or rapidly decreases upon differentiation from ES cells (3). Recent physical evidence supports the co-occurrence of both H3K4me3 and H3K27me3 on the same nucleosomes, and demonstrates resolution of bivalent domains upon differentiation (4). This leads to current understanding that these marks indicate genes "poised" for response to some differentiation or selective stimulus.

Aberrant gene silencing, leading to inactivation of tumor suppressors and dysregulation of cell growth, has long been regarded an important feature of carcinogenesis (5). More recently, it has been shown to play an active role in the acquisition of drug resistance driven by epigenetic and genetic mechanisms (6–8). While a large body of work in the epigenetic area focuses on methylation of cytosines in DNA (CpG methylation), recent evidence also implicates histone modifications, particularly H3K27me3, as a means of aberrant gene silencing in cancer. These two mechanisms are known to be linked (9), and genes associated with bivalent marks in ES cells are enriched in genes with promoter CpG hypermethylation in cancers (10). A further

[1]Department Surgery & Cancer, Imperial College London, London, United Kingdom. [2]Centre for Trials Research, Cardiff University, Cardiff, United Kingdom. [3]Peter MacCallum Cancer Centre, Melbourne, Victoria, Australia. [4]Institute of Cancer Research, Sutton, United Kingdom.

Note: Supplementary data for this article are available at Cancer Research Online (http://cancerres.aacrjournals.org/).

Corresponding Author: Robert Brown, Imperial College London, IRDB 1st Floor, Hammersmith Hospital, London W12 0NN, United Kingdom. Phone: 4420-7594-1804; Fax: 4420-7594-2129; E-mail b.brown@imperial.ac.uk

doi: 10.1158/0008-5472.CAN-17-1650

observation linking PRC2 with cancer, and particularly to cancer stem cells, is that the histone methyltransferase component of PRC2, EZH2, is overexpressed in tumor-initiating subpopulations of ovarian cancer cell lines, and inhibition of EZH2 inhibited tumor growth (11). High EZH2 expression has been associated with poor outcomes in a range of cancer types (12, 13).

We previously showed that a primary high-grade serous ovarian tumor had bivalent chromatin domains enriched for loci that are bivalently marked in ES cells, but additionally at loci detected only in the tumor (14). These bivalently marked genes were preferentially silenced in tumor-initiating subpopulations of an ovarian cancer cell line and in the platinum-resistant isogenic pair of a platinum-sensitive ovarian cancer cell line. This suggests that the acquisition of stem cell–associated bivalent chromatin domains could provide tumor cells a mechanism for rapid adaptation to drug exposure, with expression changes made more persistent through acquisition of DNA methylation. The involvement of these epigenetic alterations in cancer cell populations may result from adaptation of normal cellular differentiation involved in tissue maintenance and regeneration, and could link the process of tumor initiation to later acquired drug resistance (15). It is therefore relevant that definitive stem cell populations from both ovarian and fallopian tube epithelia have recently been characterized (16).

We have now generated histone modification profiles from further primary high-grade serous ovarian tumors and from normal ovarian tissue in an attempt to shed light on the role of bivalent chromatin domains in ovarian carcinogenesis and acquired drug resistance in patients. A schematic summary of our approach and our key findings are shown in Fig. 1. As would be expected, there is variation in the sets of H3K27me3 and H3K4me3 marked genes from tumor to tumor. However, we show that the expanded common set of genes bivalently marked in ovarian tumors is strongly enriched for the canonical PRC2 target genes associated with differentiation. Importantly, we use paired tumor samples taken from a cohort of patients before and after the acquisition of platinum resistance to show that these bivalently marked PRC2 target genes are predisposed toward epigenetic silencing via gain of DNA methylation following chemotherapy, during acquired drug resistance of patients' tumors.

Materials and Methods

Sample collection and cell lines

Four high-grade serous epithelial ovarian tumor samples from untreated patients at primary presentation, three normal ovarian surface epithelium samples, and one normal fallopian tube epithelium sample were approved and obtained from the "HTA-approved" Imperial College Healthcare NHS Trust Tissue Bank (authorized by the Wales MREC). Tumor collection and analysis for this study was approved by the West London Research Ethics Committee (reference 09/H0707/89) according to Declaration of Helsinki. Written consent was obtained from all patients included in this study who provided tumor tissue for research.

PEA1 and PEA2 cell lines (17) were obtained and used within 6 months from Department of Surgery and Cancer cell stocks. STR profiling was used to authenticate cell lines prior to freezing and to confirm that pairs of lines were related. All cell lines were mycoplasma free and checked fortnightly.

Chromatin immunoprecipitation, sequencing, and PCR

All chromatin immunoprecipitation (ChIP)-seq sample processing and library preparation was performed as described previously (14). ChIP libraries were sequenced using an Illumina HiSeq2000 at the CSC Genomics Core Laboratory of Imperial College London. Individual 50-bp reads were filtered if they contained 5 base calls with quality Phred score less than 30, or

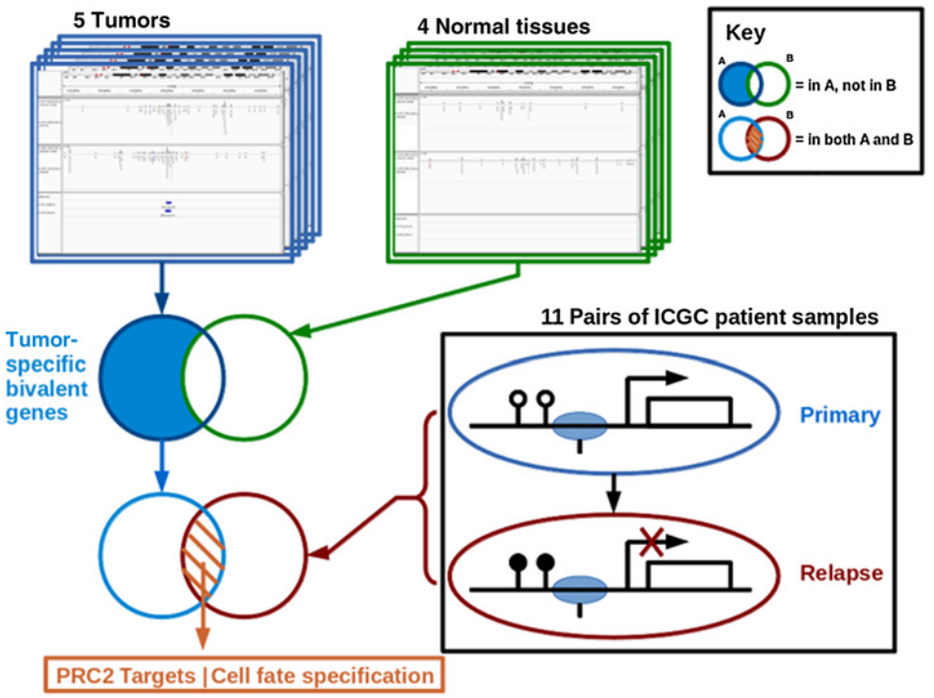

Figure 1.
Graphical summary of analytic approach and key findings. ChIP-seq for H3K27me3 and H3K4me3 (in comparison with input DNA) was used to obtain genome-wide bivalent mark profiles in 4 primary ovarian tumors and 4 normal tissue samples, supplemented by the profile from a primary ovarian tumor obtained from our previous study. Genes with both H3K27me3 and H3K4me3 marks within 2 kb of the TSS in any of the tumors, but none of the normal tissues were taken forward as representative of poised genes in primary ovarian cancers. These genes systematically gained methylation and reduced expression in ovarian cancer patient samples obtained at relapse following cytotoxic chemotherapy treatment, relative to their primary tumor samples. The set of genes that was both poised in primary tumors and epigenetically silenced upon relapse was strongly enriched for regulators of differentiation, including the classical ES cell Polycomb targets.

if they contained any undetermined bases. The remaining reads were mapped to the hg19 reference genome using Bowtie2 (18). Reads were further filtered so that a maximum of one uniquely mapped read was kept for each genomic coordinate. All reads mapping to the DAC Consensus Excluded Regions were discarded and cross-correlation for each filtered sequence library was calculated as described (19) across a range of interstrand offsets from 1- to 200-bp, at 5-bp intervals. Locations of significant peaks of enriched DNA in each of the ChIP samples were identified using MACS v1.4.2 (20) using a *P* value cutoff of 1e−4.

Immunoprecipitation enrichment of candidate regions was confirmed through qPCR of ChIP from the high-grade serous ovarian cancer cell line PEA1. Cells were crosslinked with 1% formaldehyde and processed according to ref. 21. Briefly, chromatin extract were sonicated using a Diagenode sonicator using 20 cycles (30-second on and 30-second off) at maximum intensity. Purified chromatin was then immunoprecipitated using 4 μg of H3K4me3 (Abcam 8580) or H3K27me3 (Abcam 6002) antibodies per ChIP. Nonimmunoprecipitated chromatin was used as Input control. PCR primer sequences are given in Supplementary Table S1. Immunoprecipitation enrichment was calculated as $\frac{\text{input\_DNAconc}}{\text{ChIP\_DNAconc}} 2^{-\Delta C_t}$, where ΔC_t denotes the difference in amplification C_t values between input DNA and antibody pull-down DNA.

Assessing differential methylation and expression in clinical samples

All DNA methylation data were taken from ovarian tumor and ascites samples from the International Cancer Genome Consortium (ICGC) study (22) profiled on the Illumina 450k HumanMethylation arrays. Eleven paired primary-relapse samples were available from which the primary sample was tumor but the paired relapse sample was from ascites, and 1 pair where tumor material from relapse was also obtained. In addition, 3 pairs of tumor and ascites samples both taken at primary presentation were available. To account for tissue-specific methylation differences between tumor cells and ascites, differential methylation was evaluated in terms of the fold increase in methylation M-values between primary and relapse samples for each pair, divided by the average fold-increase in methylation M-values between tumor and ascites pairs. For differential gene expression, log-transformed, normalized FPKM RNA-seq counts were obtained for each gene from the ICGC ovarian cancer study (22). Statistics for differential expression were calculated using LIMMA (23) with a linear model term for each patient, a term to model tissue-specific differences and a term to model differences from primary to relapse. Empirical Bayes moderated *t*-statistics were obtained for the primary-versus-relapse coefficient for each gene.

Bisulphite pyrosequencing

A total amount of 500 ng of genomic DNA was bisulphite modified using the Zymo Research EZ-DNA Methylation Kit (Cambridge Bioscience) according to the manufacturer's instructions. Sequences of pyrosequencing primer sets are provided in Supplementary Table S1. Pyrosequencing PCR was performed in duplicate for each sample in a 25 μL volume containing an end concentration of 1 U Faststart Taq polymerase (Roche), 1× FastStart PCR Buffer including 2 μmol/L $MgCl_2$ (Roche), 0.05 mmol/L dNTPs (Roche), 0.4 μmol/L primers (each) adding 1 μL of modified DNA template using the following conditions: 95°C for 6 minutes, 45 cycles of 95°C for 30 seconds, 58°C for 30 seconds, 72°C for 30 seconds, followed by 72°C for 5 minutes and terminating at 4°C. Pyrosequencing of PCR products was performed on PyroMark Q 96 MD using the PyroGold Reagent Kit (Qiagen) according to the manufacturer's instructions. The methylation percentage of CpG sites for individual genes was calculated by using the Pyro Q-CpG software (version 1.0.9), Biotage.

Statistical analysis

Hypergeometric test refers to use of the hypergeometric distribution in **R** to calculate the probability of at least as great an observed overlap between two sets of genes occurring purely by chance.

Pearson correlation coefficients and their corresponding significance estimates were calculated in **R**.

The "GeneSetTest" function in the Limma package (23) from Bioconductor was used to evaluate the statistical significance of a systematic shift of a set of genes towards an increase (or decrease) in measurements between two groups of samples measured in a molecular profiling experiment.

Module Maps (24) were used to create signature scores for each sample, summarizing the level of gene expression or DNA methylation across a set of genes or CpG loci, respectively. Functional annotation of poised, hypermethylated genes was carried out using DAVID according to described protocol (25).

Assessment of statistical significance of observed increase in DNA methylation estimates from pyrosequencing of PEA1 and PEA2 cell lines was performed using the binomial distribution implemented in R, with null hypothesis based on an assumed probability of 0.5 of each locus showing higher methylation in PEA2 than PEA1.

Availability of data and material

ChIP-seq data for 4 primary tumor samples and 4 normal tissue samples, along with microarray data from 4 primary tumor samples, will be made available through Gene Expression Omnibus (GSE107931). RNA-seq and DNA methylation data from ICGC ovarian cancer patients at primary presentation and relapse are available from the ICGC Data Portal (https://icgc.org/icgc/cgp/67/304/809). All processed datasets, annotation resources, and data analysis code will be made available for public access on the first author's Imperial College website (http://www.imperial.ac.uk/people/e.curry).

Results

Bivalent chromatin marks in primary ovarian tumors associate with gene silencing

Chromatin was extracted from 4 primary high-grade serous ovarian tumors, 3 healthy ovarian surface epithelium samples, and 1 fallopian tube epithelium sample. Following extraction, ChIP) in conjunction with high-throughput sequencing (ChIP-seq) was performed (as described in Materials and Methods) to identify genome-wide positioning of the permissive histone mark H3K4me3 and the repressive mark H3K27me3. Regions of significant enrichment of IP over input DNA control, referred to as "peaks," were computed for each sample and each histone mark using MACS (20). Genes with peaks in both active and repressive histone marks lying within 2-kb of their TSS were called bivalently marked. All samples showed evidence of bivalent promoters, with all tumor samples showing significantly more genes carrying bivalent marks than would be expected from random overlap of

the individual active and repressive marks (see Supplementary Information). The number of bivalently marked genes in each sample is markedly correlated (Pearson correlation coefficient 0.856, $P = 0.0067$) to the number of genes marked with H3K27me3 in each sample, but not H3K4me3. That is, samples with more bivalently marked genes tend to have more H3K27me3-marked genes, but not more H3K4me3-marked genes, than samples with fewer bivalently marked genes. This suggests that the H3K27me3 mark is more critical in creating the bivalent chromatin state, supporting the well-established links between PRC2 and repression of gene expression at bivalent promoters. It also suggests that the set of bivalently marked genes in each profiled tissue is only a subsample of the full complement that could have been observed. This motivated us to identify regions of the genome that show a disposition toward bivalency across multiple tumors but not in the normal tissue samples.

Combining this with the set of bivalently marked genes from a previous experiment (14) gave us a list of genes with evidence for poised promoter chromatin states in multiple primary high-grade serous ovarian tumors, but not in normal ovarian surface or fallopian epithelia (provided in Supplementary Table S2).

Previous work showed that genes with bivalent promoters were more likely to be transcriptionally silenced in the profiled tumor than genes with active promoter marks (14). Applying the same analysis strategy to gene expression microarray data obtained from the tumors that were used for ChIP-seq profiling of bivalent chromatin, the average proportion of present, marginal, and absent detection calls for all probe-sets mapping to bivalently marked genes were compared against the proportions for probe-sets mapping to genes with H3K4me3 mark only. Genes with bivalently marked promoters were significantly less likely to be expressed at a detectable level (χ^2 test $P < 2.2e{-}16$), suggesting that the set of bivalently marked genes are representative of a degree of functional epigenetic silencing.

Poised genes in primary tumors are enriched for regulators of cell fate

Genes marked with bivalent promoters in ES cells are considered to be key determinants of differentiation pathways, being in a poised state that retains the capacity to either increase or decrease transcription rates rapidly when required. The genes harboring proximal bivalent chromatin domains in the ovarian tumors analyzed are highly enriched for Polycomb targets with poised promoters in ES cells (hypergeometric test $P = 5.8e{-}100$, PRC2 targets obtained as mentioned in ref. 26). Although the cell of origin of serous ovarian cancers remains contentious with both ovarian surface and fallopian tube epithelia being suggested (27, 28), a recent study provided molecular characterization of a definitive ovarian and fallopian tube epithelial stem cell population in the mouse, marked by expression of Lgr5 (16). The set of genes with bivalently marked chromatin in the ovarian tumor samples was significantly enriched for human orthologs of genes that were downregulated in the $Lgr5^+$ stem cell compartment relative to $Lgr5^-$ comparison (hypergeometric test, $P = 0.006$). As there was no such enrichment for orthologs of the genes upregulated in $Lgr5^+$ cells, it would appear that repression of transcription of genes marked with bivalent chromatin in ovarian tumor cells would keep the cells in a more "stem cell–like" state, but maintaining the capacity to lose stem cell–associated features rapidly as and when required. Table 1 displays a summary of the numbers of genes in each set.

Table 1. Summary of numbers of genes with bivalent marks in ovarian tumor and normal tissues

Tissue source	Bivalently marked genes	ES Polycomb targets[a] (out of 1,567)	Ovarian Lgr5 targets[b] (out of 203)
Ovarian tumor	747	217	11
Normal (OSE, FT)	207	23	3

[a]Previously described Polycomb targets in ES cells (26).
[b]Orthologs of genes downregulated in $Lgr5^+$ mouse ovary cells (16).

Bivalent chromatin domains and DNA hypermethylation during acquisition of drug resistance

To examine the hypothesis that bivalent promoters in tumors at presentation may predispose genes towards hypermethylation during acquisition of drug resistance, we have integrated our ChIP-seq data with RNA expression and DNA methylation data generated by the ICGC of high-grade serous ovarian cancer, including paired samples from patients both at primary, chemo-naïve, presentation, and upon relapse following platinum-based chemotherapy (22). It has previously been shown that key differentiation genes bivalently marked with promoters in ES cells are predisposed toward hypermethylation during tumor development (10, 29). Consistent with this, the set of promoters we identify that have hypermethylation in primary tumors relative to normal fallopian tube tissue samples show enrichment for ES Polycomb target genes (Limma gene set test, $P = 0.01$). Furthermore, we see an enrichment of the ES Polycomb targets among the set of genes, which gains promoter CpG methylation at drug-resistant relapse compared with primary chemo-naïve tumors (hypergeometric test, $P = 2.1e{-}08$). These ES Polycomb target genes also show a systematic downregulation of gene expression from primary to relapse samples (Limma gene set test, $P = 6.0e{-}10$). Genes with proximal CpG loci gaining methylation, compared with all genes, show a significant systematic downregulation of gene expression from primary to relapse samples (Limma gene set test $P = 3.5e{-}05$), arguing that the gain of DNA methylation is associated with the reduction in expression.

To evaluate systematic changes of promoter CpG methylation following chemotherapy across genes marked with bivalent chromatin domains in primary, chemo-naïve, ovarian tumor cells, we calculated the average change in CpG methylation between matched primary and relapse samples from the same patient. Comparing the corresponding distribution for loci in bivalently marked promoters with that of all promoter CpGs, we see a systematic shift toward greater hypermethylation (t test $P = 0.036$; Supplementary Fig. S1). We computed Module Map scores (24) to summarize promoter CpG methylation across entire gene sets in each sample for illustration in the heatmap in Fig. 2A, with average module map scores across primary and relapse samples shown in Fig. 2B. To further demonstrate that this effect was due to more hypermethylation and not less hypomethylation, we extracted only those loci with greater than 2-fold average increase in methylation in relapse samples compared with primary tumors (given in Supplementary Table S3), and found that this set was enriched for the set of promoters with bivalent chromatin domains identified by ChIP-seq in primary ovarian tumors (hypergeometric test, $P = 0.004$). Functional annotation of the list of genes that are both bivalently marked and show at least 2-fold increase in DNA methylation upon

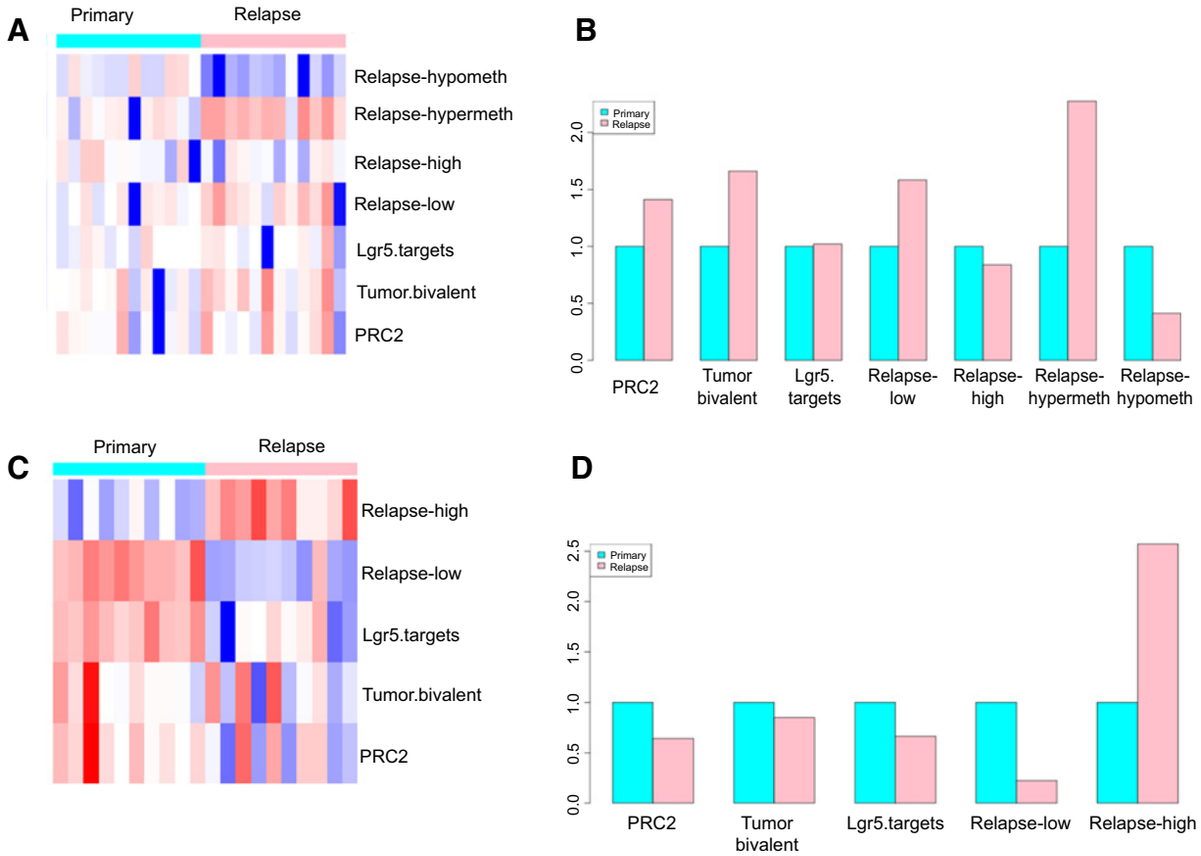

Figure 2.

Module maps summarizing DNA methylation and gene expression signatures. Heatmaps show module map scores for gene sets in terms of DNA methylation (**A**) and gene expression (**C**) in individual primary tumor and relapse ascites samples from the ICGC high-grade serous ovarian cancer cohort. DNA methylation module map scores $\log_2$ transformed in **A**. Set of genes with bivalent chromatin domains in ovarian tumors is labeled "tumor.bivalent," set of polycomb targets in ES cells is labeled "prc2," set of orthologs of genes repressed in Lgr5$^+$ mouse ovary stem cells is labeled "lgr5.targets," sets of genes up- and downregulated in expression in relapse ascites relative to primary tumors are labeled "relapse.hi" and "relapse.lo," respectively, and sets of genes hyper- and hypomethylated in relapse ascites relative to primary tumors are labeled "relapse.hyper" and "relapse.hypo," respectively. Color bar along top of the heatmaps indicates primary samples with blue and relapse samples with pink. Average module map scores across all primary samples (blue) and all relapse samples (pink) are shown in bar charts for DNA methylation (**B**) and for gene expression (**D**). These show that methylation tends to increase in relapse for the genes with bivalent marks in primary ovarian tumors, for the polycomb targets in ES cells, and for genes decreasing expression on relapse. Methylation tends to decrease in relapse for the genes increasing expression on relapse. Gene expression shows the opposite trend, decreasing for the genes with bivalent marks in primary ovarian tumors and for the Polycomb targets in ES cells.

relapse suggests a link between this hypermethylation and a suppression of cellular differentiation (GO terms "pattern specification process" and "cell fate commitment" were enriched with adjusted P values 7.2e-8 and 1.9e-4, respectively, a full table of enriched GO terms is provided in Supplementary Table S4). Some of the samples are observed to have clearer systematic promoter hypermethylation of these target genes than others. In fact there is considerable heterogeneity, both within the primary and the relapse tumors, in the levels of DNA methylation for even the gene set representing the most consistently differentially methylated between the groups. This may arise from multiple alternative mechanisms for silencing being employed in the tumors, as found in ref. 30.

In primary tumor and relapse pairs taken from the ICGC patient cohort ($n = 10$), gene expression profiling by RNA-seq data shows a systematic downregulation of the set of genes marked with bivalent chromatin domains in primary ovarian tumor cells (Limma gene set test, $P = 0.037$). We computed Module Map scores to summarize expression levels across entire gene sets in each sample for illustration in the heatmap in Fig. 2C, with average module map scores across primary and relapse samples shown in Fig. 2D. Interestingly, we also see that the orthologs of Lgr5-downregulated genes in the mouse ovarian stem cell model show a strong systematic downregulation of expression in relapsed samples relative to primary tumors (Limma gene set test $P < 1e{-}12$). This latter observation implies that tumor cells upon relapse have a more stem cell–like gene expression profile and that bivalent chromatin marks may provide a mechanism for the observation that high-grade serous ovarian cancer cells enhance stem cell–like characteristics following exposure to chemotherapy (10, 11). The individual PRC2 complex members *EZH2*, *EED*, and *SUZ12* all showed higher median expression in the relapse samples relative to primary samples, but this difference was only statistically significant in the case of *SUZ12* (paired t test $P =$

0.025). Furthermore, we saw significant overexpression of *DNMT3B* ($P = 0.047$), which suggests that transcriptional upregulation of this *de novo* DNA methyltransferase may be involved mechanistically in the observed epigenetic silencing of bivalently marked genes.

We computed the difference in average promoter methylation and the difference in expression for each gene in each pair of primary relapse samples. These differences were negatively correlated (Pearson correlation $= -0.05$, product moment test, $P = 0.002$), indicating increases in promoter methylation tending associating with decreases in expression. The set of bivalently marked genes showed on average a greater increase in methylation and greater decrease in expression between primary and relapse samples than other genes (t test, $P = 0.09$ and $P = 0.08$, respectively). The absolute promoter methylation levels of bivalent genes were similarly distributed to those of all other genes, but with more frequent occurrence of methylation >10% (Supplementary Fig. S2). This relationship was observed in both primary and relapse samples.

To suggest key pathways affected by the epigenetic change during chemotherapy and relapse, we computed the average change in promoter methylation and gene expression across all bivalently marked genes in pathways from the Consensus Pathway Database (31), from primary to relapse samples. A significant negative correlation was observed at the pathway level between change in methylation and change in expression (Pearson correlation coefficient $= -0.2$, $P < 2 \times 10^{-16}$). We noted systematic increases in methylation and decreases in expression of genes in "BMP signaling" and "MicroRNAs in cancer" pathways (Supplementary Fig. S3). miRNA signaling has previously been demonstrated to be regulated through DNA methylation (32) and implicated in drug resistance (33) in ovarian cancer. BMP signaling is known to regulate differentiation (34), and less differentiated stem cells are known to be more resistant to chemotherapy (35). These observations therefore suggest possible mechanisms relating to the acquired drug resistance observed in these relapsed tumors.

A set of candidate loci from the bivalently marked genes showing hypermethylation on relapse were selected for independent evaluation in the PEA1/PEA2 isogenic cell line pair (17). Bivalent marks at promoters for *DXL5*, *TRIM7*, *CYP21B1*, and *HOXD10* in the primary tumor–derived cell line PEA1 were confirmed through ChIP-qPCR. Fold enrichment from immunoprecipitation with antibodies targeting each of H3K4me3 and H3K27me3, relative to input DNA, is shown in Fig. 3A. All selected loci show marked enrichment of the target regions

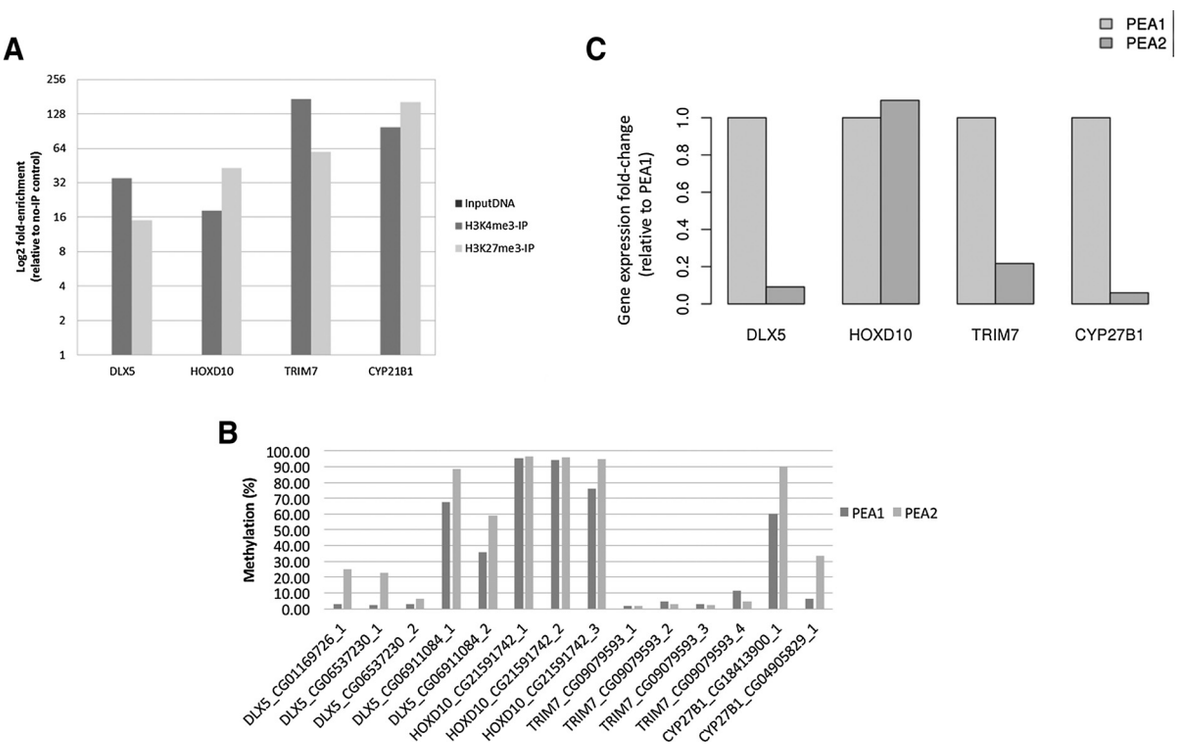

Figure 3.

Evaluation of bivalent chromatin marks and hypermethylation in PEA1/PEA2 ovarian cancer cell line model. **A,** Fold enrichment from H3K4me3 and H3K27me3 immunoprecipitation of PEA1 cell line DNA at promoter regions of candidate genes, based on ChIP-qPCR quantification. Each IP shown is an average of two independent chromatin extractions, pull-down and amplification. Values shown reflect concentration of target region DNA relative to all DNA in the sample, normalized to no-IP input DNA. **B,** Quantification of promoter CpG methylation levels in PEA1 and PEA2 cell lines by bisulphite pyrosequencing. Values shown represent proportion of sequenced DNA fragments with the corresponding CpG site methylated out of all sequenced DNA fragments mapping to that CpG site. Each assay reflects the average of three independent DNA extractions. **C,** Quantification of gene expression levels in PEA1 and PEA2 cell lines from RNA-seq. Values shown represent the number of reads mapped to each gene relative to number of reads mapping to GAPDH in each of three replicates.

through both H3K4me3 and H3K27me3 ChIP. Levels of DNA methylation for CpG sites in these promoters were assayed through bisulphite pyrosequencing, in both primary tumor–derived cell line PEA1 and the cell line PEA2, which was derived from the same patient as PEA1 but after chemotherapy and subsequent relapse (17). Methylation levels (an average of three replicates) for these CpG sites are presented in Fig. 3B, showing an increase in methylation in PEA2 relative to PEA1 for 11 of the 14 loci. Assuming under randomness that each CpG site would have a 50% chance of being measured at a higher level in PEA2 relative to PEA1, we have $P = 0.02$ for seeing at least that many loci hypermethylated in PEA2 purely by chance. Of the 4 genes tested, only *TRIM7* did not feature at least 1 CpG site with >10% increase in methylation. This independent evaluation supports the systematic promoter hypermethylation of bivalently marked genes that we established on the basis of analysis of patient samples. To relate changes in DNA methylation to changes in gene expression, we mapped RNA-seq reads from the PEA1 and PEA2 cell lines to these candidate genes and normalized to the number of reads mapping to *GAPDH* in each replicate (coordinates and counts given in Supplementary Table S5). Figure 3C shows 3 of the 4 genes markedly downregulated in PEA2, and a systematic decrease across the entire bivalently marked gene set (Wilcoxon signed rank test $P < 2 \times 10^{-16}$) is observed, confirming a general trend for silencing of these genes following exposure to chemotherapy.

Discussion

We previously proposed a model in which overexpression of EZH2 in cancer cells, particularly those with lower proliferation rate and greater tumorigenic capacity, leads to aberrant marking of promoters with bivalent chromatin domains, predisposing these loci to epigenetic silencing via DNA methylation during the course of tumor evolution toward an acquired drug-resistant state (15). We previously presented evidence of bivalent chromatin domains in a primary ovarian tumor, showed that these were enriched for Polycomb targets associated with developmental regulation, and linked the bivalently marked genes to transcriptional silencing in tumor-initiating cell–enriched subpopulations and chemotherapy-resistant models of ovarian cancer cell lines (14). However, access to paired tissue samples from patients prior to and after exposure to chemotherapy in our current study allowed us to demonstrate systematic epigenetic silencing of bivalently marked gene sets occurring in patients in the course of treatment. During this time, the cancer cells have been exposed to platinum-based chemotherapy and have both regrown a tumor mass and altered their drug sensitivity so that the same cytotoxic chemotherapy is less effective at therapeutic doses. While genetic change such as reversion of Brca1 mutations are important in drug resistance and treatment failure at relapse, epigenetic change such as DNA methylation also has a key role (6, 36). We observe bivalent genes defined from primary HGSOC tumors compared against normal ovarian and tubal epithelia, and to canonical Polycomb targets defined in ES cells, which gives assurance that the gene sets analyzed are not overly dependent on data from individual subjects. Given that we see lower expression of Lgr5-downregulated orthologs in relapse tissue, and functional annotation of the genes found to be bivalently marked and hypermethylated upon release points to a signature associated with cell fate specification, we believe that epigenetic reprogramming associated with drug-resistant relapse could reflect a more stem-like phenotype through suppression of differentiation. Alternatively, it may be that stem cells and tumor cells share common mechanisms of poised chromatin states. Thus, cancer cells may also be using the regulation of poised chromatin states to flexibly respond to selective pressures allowing increased plasticity. It can be seen that there is variability in the extent of hypermethylation of these gene sets, with some patients showing greater increases in methylation between primary and relapse than others. This cohort is too small to consider whether there are clinical implications of the extent of hypermethylation of bivalently marked genes, but this would be interesting to investigate should methylation profiles be obtained from more paired samples.

With available data, we cannot differentiate between poised states leading to the acquisition of silencing during chemotherapy, as opposed to bivalently marked loci already being fully silenced in (drug-resistant) clones within the primary tumor sample, which survived and grew out following initial treatment to form the relapse. The only way to address this definitively would be to use single-cell genetic and epigenetic profiling of all tumor samples, which remains technically infeasible at this time. It also remains to be demonstrated whether or not any of the epigenetic silencing events we have observed are directly contributing to the functional acquisition of drug resistance in high-grade serous ovarian cancer cells, although our set of genes with bivalent promoters in tumors included *FLNC* and *MDK*, previously identified key drivers of epigenetically mediated acquisition of drug resistance in ovarian tumor cell line models (6). Proof of a direct causal link would require further experimental evidence. Such experiments would require emergence of epigenetic editing technology (e.g., ref. 37) to induce the presence or absence of bivalent marks at PRC2 target gene promoters, then follow an appropriate model through acquisition of drug resistance, monitoring changes to DNA methylation and gene expression. As such technology is still in development, experimental proof of causality is beyond the scope of this study.

Importantly, we have shown that the histone modification profile from a primary tumor at initial clinical presentation is informative of the DNA methylation and gene expression state of drug-resistant tumor at relapse many months after treatment. This suggests that drug-resistant disease could theoretically be targeted before it develops, through a personalized medicine strategy that utilizes epigenetic profiles obtained from a primary tumor sample to predict the most likely drivers of subsequent resistance. One can imagine a situation in which the bivalent chromatin profile of a tumor is mapped and used to select, from a list of available therapeutics targeting genes or pathways known to cause chemotherapy resistance, those with targets most likely to become altered during disease relapse. Alternatively, it may be the case that the epigenetic silencing events are acquired during chemotherapy and only in a poised state at presentation, a scenario that might be implied by the observation of overexpression of the PRC2 complex member *SUZ12* and the *de novo* DNA methyltransferase *DNMT3B* on drug-resistant relapse. The emergence of chemotherapy resistance is facilitated by the ability of cancer cells to alter their epigenetic landscape, particularly via controlling bivalent chromatin domains and DNA methylation. Treating patients with drugs that target these processes, either along with chemotherapy or in a maintenance setting during remission, could prevent the cancer cells from adapting their epigenetic landscape to acquire chemotherapy resistance.

We have shown here that ovarian tumor cells harbor the bivalent chromatin domains that are characteristic of pluripotent cells held in an undifferentiated state poised to undergo rapid phenotypic change on lineage commitment. Specifically, we see poised chromatin states leading to epigenetic silencing of genes involved in stem cell differentiation, implying this disruption of normal differentiation processes as a potential mechanism by which tumor cells could adapt to the presence of cytotoxic chemotherapy and that common mechanisms give rise to drug-resistant populations as observed during normal cell differentiation. Promoters kept in a poised state by the presence of these domains would enable cells not immediately killed by cytotoxic chemotherapy to adapt to the changes in their environment brought about by this treatment, and repopulate a tumor with cells reprogrammed to suppress cellular mechanisms of drug sensitivity and treatment response. While we observe these similarities of ovarian cancer cells to ovarian stem cells, we do not have data to assess the extent to which cancer cells derive from stem cells. It would be possible for these cells to use alternative mechanisms of establishing and maintaining bivalent chromatin domains, and that these could be located in different positions throughout the genome. Lineage tracing experiments to investigate tumor formation from Lgr5-expressing cells would be of interest to us, but beyond the scope of this study. In this context, we highlight the observation that mouse $Lgr5^{+}$ stem cells of the ovary and fallopian tube overexpress Ezh2 relative to the Lgr5-differentiated ovarian and tubal epithelia (16). Tumor-initiating subpopulations of human cancer cell lines with stem cell–like properties also overexpress EZH2 relative to nontumor–initiating subpopulations (11). If both the normal adult stem cell compartment of the ovary and tumor-initiating cells of ovarian cancers overexpress the enzyme responsible for deposition of the H3K27me3 histone mark, which is a key step in formation of bivalent chromatin domains, it may suggest that this mechanism is already present in the normal physiology of the ovary. This, in turn, would indicate that high-grade serous ovarian cancers are physiologically disposed toward this capacity for epigenetically driven acquired drug resistance. We speculate that therapeutics targeting aberrant PRC2 activity in tumor cells during remission, such as histone methyltransferase inhibitors, could prevent acquisition of resistance by DNA methylation to widely used cytotoxic chemotherapies and offer a means of preventing drug resistance emergence.

In conclusion, we have shown that high-grade serous ovarian cancer at initial presentation have bivalently marked chromatin domains, containing active H3K4me3 and repressive H3K27me3 histone marks, which define gene sets that are more likely to have increased promoter CpG methylation and reduced gene expression at patient relapse with resistant disease. This provides the first evidence from patient samples that epigenetic silencing during acquired drug resistance could be underpinned by pre-existing histone modifications associated with genes being in a poised state.

Disclosure of Potential Conflicts of Interest

No potential conflicts of interest were disclosed.

Authors' Contributions

Conception and design: E. Curry, S. Ghaem-Maghami, D.D.L. Bowtell, R. Brown

Development of methodology: E. Curry

Acquisition of data (provided animals, acquired and managed patients, provided facilities, etc.): C. Zeller, D. Patten, J. Gallon, C.S. Wilhelm-Benartzi, S. Ghaem-Maghami, R. Brown

Analysis and interpretation of data (e.g., statistical analysis, biostatistics, computational analysis): E. Curry, D. Patten, J. Gallon, C.S. Wilhelm-Benartzi, R. Brown

Writing, review, and/or revision of the manuscript: E. Curry, C.S. Wilhelm-Benartzi, S. Ghaem-Maghami, D.D.L. Bowtell, R. Brown

Administrative, technical, or material support (i.e., reporting or organizing data, constructing databases): E. Curry, N. Masrour, D. Patten, S. Ghaem-Maghami, D.D.L. Bowtell

Study supervision: S. Ghaem-Maghami, R. Brown

Acknowledgments

This study was supported by a Cancer Research UK grant (A13086), Ovarian Cancer Action Research Centre, Imperial Experimental Cancer Medicine Centre, and the Imperial NIHR Biomedical Research Centre. Tissue samples were provided by the Imperial College Healthcare NHS Trust Tissue Bank. We would like to acknowledge support of the ICGC Ovarian Cancer study group for access to data from clinical samples. We would like to thank Erick Loomis for comments on the manuscript.

The costs of publication of this article were defrayed in part by the payment of page charges. This article must therefore be hereby marked *advertisement* in accordance with 18 U.S.C. Section 1734 solely to indicate this fact.

Received June 6, 2017; revised October 12, 2017; accepted January 10, 2018; published OnlineFirst January 16, 2018.

References

1. Cao R, Wang L, Wang H, Xia L, Erdjument-Bromage H, Tempst P, et al. Role of histone H3 lysine 27 methylation in Polycomb-group silencing. Science 2002;298:1039–43.
2. Pauler FM, Sloane MA, Huang R, Regha K, Koerner MV, Tamir I, et al. H3K27me3 forms BLOCs over silent genes and intergenic regions and specifies a histone banding pattern on a mouse autosomal chromosome. Genome Res 2009;19:221–33.
3. Fisher CL, Fisher AG. Chromatin states in pluripotent, differentiated, and reprogrammed cells. Curr Opin Genet Devel 2011;21:140–6.
4. Voigt P, LeRoy G, Drury WJ, Zee BM, Son J, Beck DB, et al. Asymmetrically modified nucleosomes. Cell 2012;151:181–93.
5. Baylin SB, Jones PA. A decade of exploring the cancer epigenome — biological and translational implications. Nat Rev Cancer 2011;11:726–34.
6. Zeller C, Dai W, Steele NL, Siddiq A, Walley AJ, Wilhelm-Benartzi CSM, et al. Candidate DNA methylation drivers of acquired cisplatin resistance in ovarian cancer identified by methylome and expression profiling. Oncogene 2012;31:4567–76.
7. Huang S, Benavente S, Armstrong EA, Li C, Wheeler DL, Harari PM. p53 modulates acquired resistance to EGFR inhibitors and radiation. Cancer Res 2011;71:7071–9.
8. Zhang S, Huang W-C, Li P, Guo H, Poh S-B, Brady SW, et al. Combating trastuzumab resistance by targeting SRC, a common node downstream of multiple resistance pathways. Nat Med 2011;17:461–9.
9. Cedar H, Bergman Y. Linking DNA methylation and histone modification: patterns and paradigms. Nat Rev Genet 2009;10:295–304.
10. Easwaran H, Johnstone SE, Van Neste L, Ohm J, Mosbruger T, Wang Q, et al. A DNA hypermethylation module for the stem/progenitor cell signature of cancer. Genome Res 2012;22:837–49.
11. Rizzo S, Hersey JM, Mellor P, Dai W, Santos-Silva A, Liber D, et al. Ovarian cancer stem cell-like side populations are enriched following chemotherapy and overexpress EZH2. Mol Cancer Ther 2011;10:325–35.
12. Varambally S, Dhanasekaran SM, Zhou M, Barrette TR, Kumar-Sinha C, Sanda MG, et al. The polycomb group protein EZH2 is involved in progression of prostate cancer. Nature 2002;419:624–9.

13. Kleer CG, Cao Q, Varambally S, Shen R, Ota I, Tomlins SA, et al. EZH2 is a marker of aggressive breast cancer and promotes neoplastic transformation of breast epithelial cells. Proc Nat Acad Sci 2003;100:11606–11.
14. Chapman-Rothe N, Curry E, Zeller C, Liber D, Stronach E, Gabra H, et al. Chromatin H3K27me3/H3K4me3 histone marks define gene sets in high grade serous ovarian cancer that distinguish malignant, tumour sustaining and chemo-resistant ovarian tumour cells. Oncogene 2012;32:4586–92.
15. Brown R, Curry E, Magnani L, Wilhelm-Benartzi CS, Borley J. Poised epigenetic states and acquired drug resistance in cancer. Nat Rev Cancer 2014;14:747–53.
16. Ng A, Tan S, Singh G, Rizk P, Swathi Y, Tan TZ, et al. Lgr5 marks stem/progenitor cells in ovary and tubal epithelia. Nat Cell Biol 2014;16:745–57.
17. Langdon SP, Lawrie SS, Hay FG, Hawkes MM, McDonald A, Hayward IP, et al. Characterization and properties of nine human ovarian adenocarcinoma cell lines. Cancer Res 1988;48:6166–72.
18. Langmead B, Salzberg SL. Fast gapped-read alignment with Bowtie 2. Nat Methods 2012;9:357–9.
19. Carroll TS, Liang Z, Salama R, Stark R, de Santiago I. Impact of artifact removal on ChIP quality metrics in ChIP-seq and ChIP-exo data. Front Genet 2014;5.
20. Feng J, Liu T, Qin B, Zhang Y, Liu XS. Identifying ChIP-seq enrichment using MACS. Nat Protoc 2012;7:1728–40.
21. Schmidt D, Wilson MD, Spyrou C, Brown GD, Hadfield J, Odom DT. ChIP-seq: using high-throughput sequencing to discover protein–DNA interactions. Methods 2009;48:240–8.
22. Patch A-M, Christie EL, Etemadmoghadam D, Garsed DW, George J, Fereday S, et al. Whole–genome characterization of chemoresistant ovarian cancer. Nature 2015;521:489–94.
23. Smyth GK. Limma: linear models for microarray data. Bioinformatics and Computational Biology Solutions using R and Bioconductor: Springer-Verlag New York; 2005. p. 397–420.
24. Segal E, Friedman N, Koller D, Regev A. A module map showing conditional activity of expression modules in cancer. Nat Genet 2004;36:1090–8.
25. Huang DW, Sherman BT, Lempicki RA. Systematic and integrative analysis of large gene lists using DAVID bioinformatics resources. Nat Protoc 2008;4:44–57.
26. Lee TI, Jenner RG, Boyer LA, Guenther MG, Levine SS, Kumar RM, et al. Control of developmental regulators by Polycomb in human embryonic stem cells. Cell 2006;125:301–13.
27. Auersperg N. Ovarian surface epithelium as a source of ovarian cancers: unwarranted speculation or evidence-based hypothesis? Gynecol Oncol 2013;130:246–51.
28. Vang R, Shih IM, Kurman RJ. Fallopian tube precursors of ovarian lowand highgrade serous neoplasms. Histopathology 2013;62:44–58.
29. Ohm JE, McGarvey KM, Yu X, Cheng L, Schuebel KE, Cope L, et al. A stem cell–like chromatin pattern may predispose tumor suppressor genes to DNA hypermethylation and heritable silencing. Nat Genet 2007;39:237–42.
30. Teschendorff AE, Zheng SC, Feber A, Yang Z, Beck S, Widschwendter M. The multi-omic landscape of transcription factor inactivation in cancer. Genome Med 2016;8:89.
31. Kamburov A, Pentchev K, Galicka H, Wierling C, Lehrach H, Herwig R. ConsensusPathDB: toward a more complete picture of cell biology. Nucleic Acids Res 2011;39:D712–D717.
32. Iorio MV, Visone R, Di Leva G, Donati V, Petrocca F, Casalini P, et al. MicroRNA signatures in human ovarian cancer. Cancer Res 2007;67:8699–707.
33. van Jaarsveld MT, Helleman J, Berns EM, Wiemer EA. MicroRNAs in ovarian cancer biology and therapy resistance. Int J Biochem Cell Biol 2010;42:1282–90.
34. Winnier G, Blessing M, Labosky PA, Hogan B. Bone morphogenetic protein-4 is required for mesoderm formation and patterning in the mouse. Gen Devel 1995;9:2105–16.
35. Alvero AB, Chen R, Fu H-H, Montagna M, Schwartz PE, Rutherford T, et al. Molecular phenotyping of human ovarian cancer stem cells unravels the mechanisms for repair and chemoresistance. Cell Cycle 2009;8:158–66.
36. Swisher EM, Sakai W, Karlan BY, Wurz K, Urban N, Taniguchi T. Secondary BRCA1 mutations in BRCA1-mutated ovarian carcinomas with platinum resistance. Cancer Res 2008;68:2581–6.
37. Hilton IB, D'Ippolito AM, Vockley CM, Thakore PI, Crawford GE, Reddy TE, et al. Epigenome editing by a CRISPR-Cas9-based acetyltransferase activates genes from promoters and enhancers. Nat Biotech 2015;33:510–7.